

Communications

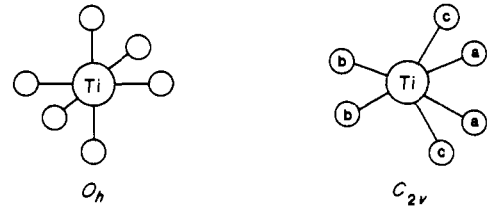
The Geometry of $[\text{TiH}_6]^{2-}$

Sir:

Current interest in organometallic complexes of high oxidation state found in the early transition metals has arisen from their implication in several important reactions, both stoichiometric and catalytic.¹ Recently a report suggested that the stable geometry of $[\text{TiH}_6]^{2-}$ was, in fact, not of octahedral symmetry but was a bicapped tetrahedron of C_{2v} symmetry² (see Figure 1). Crystal and ligand field theories both clearly predict an octahedral arrangement of the six H atoms about a central Ti, yet application of the frontier molecular orbital (FMO) theory leads to the conclusion that the stable geometry of $[\text{TiH}_6]^{2-}$ is of C_{2v} symmetry,³ and extended Hückel (EH) calculations support this result.⁴ In this communication we will argue that the lowest energy ground-state structure of $[\text{TiH}_6]^{2-}$ is octahedral and compare the predictions of various methods of electronic structure calculation, two semiempirical methods (extended Hückel,^{4,5} intermediate neglect of differential overlap (INDO)⁶ and ab initio methods using minimal (MINI)⁷ and extended basis sets (DZP).⁸

In Tables I and II are shown respectively geometries (vide infra) used with and total energies for various calculational methods. EH refers to standard extended Hückel calculations using weighted H_{ij} 's⁵ and the parameters of ref 2, MINI to ab initio calculations using the MINI basis set of Huzinaga et al.,⁷ DZP to ab initio calculations using a double ζ plus polarization basis set of Dunning⁸ for H and an augmented Wachters basis set for Ti,⁹ DZP+ to ab initio calculations with the DZP basis set extended further with the addition of a diffuse s type orbital (exponent 0.036) on H and diffuse s and p type orbitals on Ti (exponents: s, 0.009947; p, 0.029841),¹⁰ and INDO to intermediate neglect of differential

Table I. Summary of the Geometries Obtained in the MINI, INDO/1, DZP, and DZP+ Calculations



	MINI	
	O_h	C_{2v}
$r_{\text{Ti-H}}, \text{Å}$	1.6985	1.6792 (a) 1.6435 (b) 1.6844 (c)
$\theta_{\text{H-Ti-H}}, \text{deg}$	90.0	146.9779 (a) 72.3118 (b) 124.3282 (c)
	INDO/1	
$r_{\text{Ti-H}}, \text{Å}$	1.6871	$\theta_{\text{H-Ti-H}}, \text{deg}$ 90.0
	DZP	
$r_{\text{Ti-H}}, \text{Å}$	1.8409	$\theta_{\text{H-Ti-H}}, \text{deg}$ 90.0
	DZP+	
$r_{\text{Ti-H}}, \text{Å}$	1.8519	$\theta_{\text{H-Ti-H}}, \text{deg}$ 90.0
	MP2/DZP+	
$r_{\text{Ti-H}}, \text{Å}$	1.8500	$\theta_{\text{H-Ti-H}}, \text{deg}$ 90.0

Table II. Summary of Calculated Energies (in au; 1 au = 627.54 kcal/mol)

	O_h	C_{2v}
EHMO ^a	-6.518 192	-6.613 445
MINI	-847.132 801	-847.206 554
$\sum_{\text{valence}} \epsilon_i$	1.642 838	1.991 992
DZP ^a	-851.565 747	-851.532 849
$\sum_{\text{valence}} \epsilon_i$	-0.325 562	-0.083 558
INDO ^a	-6.559 485	-6.479 494
$\sum_{\text{valence}} \epsilon_i$	1.211 796	1.420 202
DZP+ (O_h opt)	-851.608 098	
$\sum_{\text{valence}} \epsilon_i$	-0.5726	
MP2/DZP+	-851.810 188	

^a These structures are calculated at the geometries obtained with the MINI basis set.

overlap calculations with the parameters of ref 6.

Two extrema, O_h and C_{2v} geometries, were obtained with the MINI basis set using Schlegel's method of geometry optimization

- (a) Koga, N.; Obara, S.; Kitaura, K.; Morokuma, K. *J. Am. Chem. Soc.* **1985**, *107*, 7109. (b) Koga, N.; Obara, S.; Morokuma, K. *J. Am. Chem. Soc.* **1984**, *106*, 4625. (c) Brookhart, M.; Green, M. L. H. *J. Organomet. Chem.* **1983**, *250*, 392. (d) Brookhart, M.; Green, M. L. H.; Pardy, R. B. A. *J. Chem. Soc., Chem. Commun.* **1983**, 691.
- Demolliens, A.; Jean, Y.; Eisenstein, O. *Organometallics* **1986**, *5*, 1457.
- Fukui, K. *Theory of Orientation and Stereoselection*; Springer-Verlag: Berlin, FRG, 1975.
- Hoffmann, R. *J. Chem. Phys.* **1963**, *39*, 1397.
- Ammeter, J. H.; Bürgi, H.-B.; Thibeault, J. C.; Hoffmann, R. *J. Am. Chem. Soc.* **1978**, *100*, 3686.
- (a) Bacon, A. D.; Zerner, M. C. *Theor. Chim. Acta* **1979**, *53*, 21. (b) Zerner, M. C.; Loew, G. H.; Kirchner, R. F.; Mueller-Westerhoff, U. T. *J. Am. Chem. Soc.* **1980**, *102*, 589.
- Huzinaga, S.; Andzelm, J.; Klobukowski, M.; Radzio-Andzelm, E.; Sakai, Y.; Tatewaki, H. *Gaussian Basis Sets for Molecular Calculations*; Elsevier: Amsterdam, 1984.
- Dunning, T. H., Jr. *J. Chem. Phys.* **1970**, *53*, 2823.
- (a) Wachters, A. J. H. *J. Chem. Phys.* **1977**, *52*, 1033. (b) Hay, J. P. *J. Chem. Phys.* **1977**, *66*, 4377. (c) Hood, D. M.; Pitzer, R. M.; Schaefer, H. F. *J. Chem. Phys.* **1979**, *71*, 705.

- (10) $[\text{TiH}_6]^{2-}$ is a doubly charged anionic species, and the MINI and DZP ab initio calculations show positive eigenvalues for occupied levels. Diffuse orbitals, s on H and s and p on Ti, were added with initial exponents of 0.036. After experimentation the exponents listed in the text were chosen on the basis of minimum energy and minimum over-saturation of the Ti s and p orbitals.

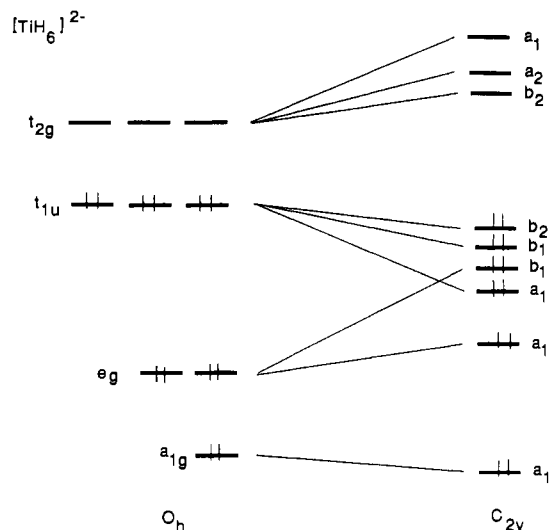


Figure 1. Orbital correlation diagram (EH) for the reduction from O_h to C_{2v} symmetry.

as implemented in the GAMESS program package^{11,12} with all gradients converged to $<5 \times 10^{-4}$ au/bohr. All of the INDO, DZP, and DZP+ geometry optimizations were started at the MINI C_{2v} structure. The INDO and DZP calculations using the method of Head and Zerner¹³ and the DZP+ calculation using Schlegel's method (GAMESS) all yielded an octahedral structure for $[\text{TiH}_6]^{2-}$. Further calculations at the level of second-order Moller-Plesset perturbation theory¹⁴ recover a correlation energy of 0.202 au and show a decrease of the Ti-H bond length of 0.0019 Å. These calculations indicate a very shallow potential energy surface for the distortion but do not alter our conclusion that the structure of $[\text{TiH}_6]^{2-}$ is octahedral. The geometries are summarized in Table I.

Application of the FMO theory to distortion of $[\text{TiH}_6]^{2-}$ leads to HOMO-LUMO mixing (t_{1u} - t_{2g}) with the resultant stabilization of the occupied orbitals derived from the HOMO (t_{1u}).³ The t_{2g} orbitals are correspondingly destabilized by this mixing, but as the orbitals are not occupied, this has no effect on the predicted energy. This situation is summarized in Figure 1.

It is perhaps not surprising that EH and FMO theory agree with one another; both entirely neglect bielectronic and nuclear repulsion, and both attribute the change in total energy to the change in the occupied orbital energy sum. While it is true in rigorous ab initio theory that, to first order, the change in the total energy caused by a change in electron density is given by the change in occupied orbital energy sum, one wonders under just what circumstances this will be true in general. Table II shows also the sum of valence orbital energies. It is noted that in all SCF methods this orbital energy sum correctly predicts the octahedral structure as the more stable. Also of interest are the orbital eigenvalues themselves. The MINI, DZP, and INDO/1 calculations all obtain at least three orbital eigenvalues, which are positive, while the DZP+ and INDO/S calculations obtain negative energies for all occupied orbitals. The INDO/S calculations are parametrized on molecular spectroscopy, rather than on molecular geometry. These last two calculations suggest that $[\text{TiH}_6]^{2-}$ might be stable in the gas phase.

If steric effects are ignored, there are two traditional mechanisms by which nonlinear molecules might achieve and maintain

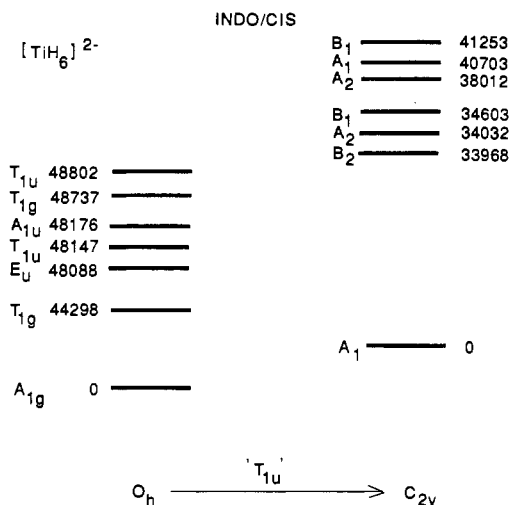


Figure 2. Calculated spectra (INDO) for O_h and C_{2v} $[\text{TiH}_6]^{2-}$ (energies in cm^{-1}).

Table III. Summary of Valence Mulliken Populations Obtained via Different Quantum-Chemical Models

		EHMO	INDO ^a	MINI	DZP (opt)
O_h	Ti	2.770	4.981	3.049	4.519 (4.430)
	H	1.538	1.170	1.492	1.247 (1.262)
C_{2v}	Ti	3.632	4.746	3.521	4.687
	H(a)	1.449	1.230	1.459	1.211
	H(b)	1.375	1.196	1.382	1.181
	H(c)	1.359	1.201	1.399	1.264

^a For this comparison the INDO wave function is deorthogonalized by assuming that it is related to an STO basis through a symmetric (Lowdin) orthogonalization.

geometries other than those expected on the grounds of simple symmetry arguments. These are the first- and second-order Jahn-Teller effects.¹⁵ The ground state of octahedral $[\text{TiH}_6]^{2-}$ is nondegenerate, and to achieve the distortion from O_h to C_{2v} via a second-order Jahn-Teller mechanism (often manifest as HOMO-LUMO mixing) there must be a low-lying excited state and a normal mode of vibration of appropriate symmetry to allow mixing with the ground state. The ground state has symmetry A_{1g} , and under O_h symmetry the 15 vibrational normal modes span the A_{1g} , E_g , T_{1u} , T_{2u} , and T_{2g} representations. The distortion shown in Figure 2 is of T_{1u} symmetry and reduces to a totally symmetric vibrational mode in C_{2v} symmetry, and so it follows that the octahedral structure is either an energy minimum or a saddle point. This second-order effect thus requires the excited-state symmetry T_{1u} , the symmetry of the HOMO-LUMO excitation ($p \rightarrow d$). But this transition is predicted to lie at high energy, 48 000 cm^{-1} , and the better calculations predict that the optimal geometry of $[\text{TiH}_6]^{2-}$ remains octahedral. The spectra calculated (INDO/S) at the two MINI basis extrema are shown in Figure 2. At the DZP+ geometry the T_{1u} excitation appears at 45 000 cm^{-1} .

In Table III we summarize the electronic populations in $[\text{TiH}_6]^{2-}$ obtained by the four quantum-mechanical techniques we have utilized, and while a direct comparison of the four methods is difficult, it does suggest some basic differences in the methods and in the basis sets. The EH, INDO, and MINI (which does not include 4p functions on titanium) calculations use a minimal basis set while the DZP and DZP+ calculations use large, extended basis sets. The formal charge on titanium in this complex is +4, and we note that the calculations which predict O_h structures, the INDO and DZP calculations, also predict considerably more electronic population on the metal than do the calculations (EH, MINI) which favor the C_{2v} structure. In the MINI calculations distortions to C_{2v} lead to an increased population on the metal, suggesting that hydride to metal charge transfer (which

- (11) Schlegel, H. B. *J. Comput. Chem.* **1982**, *3*, 214.
 (12) Dupuis, M.; Spangler, D.; Wendolowski, J. "GAMESS"; NRCC Software Catalogue; Lawrence Berkeley Laboratory, USDOE: Berkeley, CA, 1980; Program QG01.
 (13) Head, J.; Zerner, M. C. *Chem. Phys. Lett.* **1985**, *122*, 264.
 (14) Carnegie Mellon University, Frisch, M.; Binkley, J. S.; Schlegel, H. B.; Raghavachari, K.; Martin, R.; Stewart, J. J. P.; Bodrowicz, F.; Defrees, D.; Seeger, R.; Whiteside, R.; Fox, D.; Fluder, E.; Pople, J. A. "GAUSSIAN 86"; Carnegie-Mellon University: Pittsburgh, PA, 1986; Release C.

- (15) Jahn, H. A.; Teller, E. *Proc. R. Soc. London, Ser. A* **1937**, *161*, 220.

cannot happen to any great extent in the absence of Ti 4p functions) is important in stabilizing this complex and that the titanium prefers a more neutral environment. The large spatial extent of the diffuse orbitals¹⁶ make a Mulliken population analysis for the DZP+ calculation virtually meaningless, and these are not reported in the table.

The DZP, DZP+, DZP+/MP2, and INDO/1 calculations all indicate that $[\text{TiH}_6]^{2-}$ is octahedral and the distortions from octahedral symmetry, during the course of a reaction or due to agostic M–H bonding in substituted complexes,^{1,2} can occur without much cost in energy. This study, however, is motivated by the report that such a simple system as $[\text{TiH}_6]^{2-}$ violated simple and very appealing crystal field concepts. The failure of the EH calculations to predict the same geometry as do the better ab initio and INDO calculations we attribute to the failure of that method to reproduce correctly the important electrostatics that form the octahedron. In the course of this study comes reinforcement of the observation that EH total energies should never really be taken too seriously, as the theory for doing so is but very qualitative.¹⁷

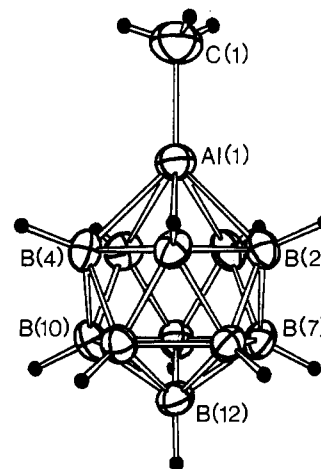


Figure 1. Molecular structure of $\text{closo-}[\text{B}_{11}\text{H}_{11}\text{AlCH}_3]^{2-}$ (ORTEP plot with 50% probability ellipsoids).

- (16) The Ti–H bond length is 1.85 Å, and for the diffuse 4s orbital on Ti (r) = 2.44 Å.
 (17) (a) Boer, F. P.; Newton, M. D.; Lipscomb, W. N. *Proc. Natl. Acad. Sci. U.S.A.* **1964**, *52*, 890. (b) Anderson, A. B.; Hoffmann, R. *J. Chem. Phys.* **1974**, *60*, 4271. (c) Anderson, A. B. *J. Chem. Phys.* **1975**, *62*, 1187.
 (18) Present address: BIOSYM Technologies, Inc., 9605 Scranton Road, Suite 101, San Diego, CA 92121.

Quantum Theory Project
 University of Florida
 Gainesville, Florida 32611

Alan D. Cameron
 George Fitzgerald¹⁸
 Michael C. Zerner*

Received March 11, 1988

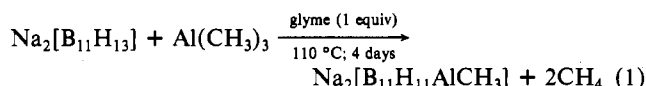
$\text{closo-}[\text{B}_{11}\text{H}_{11}\text{AlCH}_3]^{2-}$, an Aluminaborane Analogue of the $\text{closo-}[\text{B}_{12}\text{H}_{12}]^{2-}$ Dianion: Synthesis, Characterization, and Molecular Structure

Sir:

Aluminacarboranes¹ and aluminum borohydride² have been characterized in some detail. Polyhedral aluminaboranes, on the other hand, have been examined less extensively.³ There have

been no reports of polyhedral aluminaboranes that are analogues of the $\text{closo-}[\text{B}_n\text{H}_n]^{2-}$ dianions. Described herein is the high-yield synthesis, characterization, and molecular structure (Figure 1) of the 1-methyl-1-aluminaundecahydrododecaborate(2–) dianion, $[\text{B}_{11}\text{H}_{11}\text{AlCH}_3]^{2-}$, an aluminaborane analogue of the $\text{closo-}[\text{B}_{12}\text{H}_{12}]^{2-}$ dianion.

When $\text{Na}_2[\text{B}_{11}\text{H}_{13}]$ is heated in liquid $\text{Al}(\text{CH}_3)_3$ in the presence of 1 equiv of glyme, $\text{Na}_2[\text{B}_{11}\text{H}_{11}\text{AlCH}_3]$ is formed in greater than 90% yields according to eq 1. It is assumed that the glyme acts



as a catalyst by cleaving the $[\text{Al}(\text{CH}_3)_3]_2$ dimer. In the absence of glyme, even after 8 days, the reaction is not complete. Progress of the reaction is followed by measuring the CH_4 evolved. The boron-11 NMR spectrum of $\text{Na}_2[\text{B}_{11}\text{H}_{11}\text{AlCH}_3]$ in $\text{THF-}d_8$ ($\text{BF}_3\cdot\text{OEt}_2$ at 0.00 ppm) consists of the following resonances which have been assigned on the basis of a 2D $^{11}\text{B-}^{11}\text{B}$ NMR study: –17.8 ppm (d, $J = 114$ Hz), boron atoms 7–11; –18.8 ppm (d, $J = 103$ Hz), boron atoms 2–6; –25.5 ppm (d, $J = 129$ Hz), boron atom 12. The $^1\text{H}\{^{11}\text{B}\}$ NMR spectrum in $\text{THF-}d_8$ (TMS at 0.00 ppm) consists of the resonances 0.82 (B–H), 0.73 (B–H), and –0.64 ppm (C–H). Relative areas of these resonances are 6.2:5.2:3, respectively, in good agreement with the theoretical ratio 6:5:3, assuming that the signal due to the proton on the apical boron atom overlaps one of the other B–H signals.

$\text{Na}_2[\text{B}_{11}\text{H}_{11}\text{AlCH}_3]$ is air-sensitive and reacts with water, producing $\text{Na}_2[\text{B}_{11}\text{H}_{13}]$ and aluminum hydrolysis products. It also reacts with 1 equiv of methanol at 65 °C to yield $\text{Na}_2[\text{B}_{11}\text{H}_{13}]$ and unreacted $\text{Na}_2[\text{B}_{11}\text{H}_{11}\text{AlCH}_3]$. This indicates that complete cleavage of the aluminum atom from the cage is favored over the formation of species such as $\text{Na}_2[\text{B}_{11}\text{H}_{11}\text{Al}(\text{OCH}_3)]$. $\text{Na}_2[\text{B}_{11}\text{H}_{11}\text{AlCH}_3]$ does not react with diethylamine or dimethylamine. This is in contrast to the case for its carborane analogues $\text{C}_2\text{B}_9\text{H}_{11}\text{AlR}$ ($\text{R} = \text{CH}_3, \text{C}_2\text{H}_5$),^{1a} which react with THF to form $\text{C}_2\text{B}_9\text{H}_{11}\text{AlR}\cdot\text{THF}$ and with stronger bases to cleave the aluminum atom from the cage.^{1a,b} Solid $\text{Na}_2[\text{B}_{11}\text{H}_{11}\text{AlCH}_3]$ reacts with $1/3$ equiv of BCl_3 to yield only one polyhedral borane product and some unreacted starting material, as determined by boron-11 NMR spectroscopy. The product has resonances at –13.6 (d, $J \approx 179$ Hz) and –15.7 ppm (br d, $J = 148$ Hz). If excess BCl_3 is employed, a much more complex reaction mixture results with many overlapping resonances in the range –10 to –30 ppm being observed in the boron-11 NMR spectrum. During both reactions $\text{B}(\text{CH}_3)_3$ is evolved, indicating halide–alkyl exchange between BCl_3 and $\text{Na}_2[\text{B}_{11}\text{H}_{11}\text{AlCH}_3]$. The formation of $\text{B}(\text{CH}_3)_3$ and the simplicity of the boron-11 NMR spectrum indicate that the product formed when $1/3$ equiv of BCl_3 is employed may be the targeted compound, $\text{Na}_2[\text{B}_{11}\text{H}_{11}\text{AlCl}]$. Further investigation of this reaction is in progress.

- (1) (a) Young, D. A. T.; Wiersema, R. J.; Hawthorne, M. F. *J. Am. Chem. Soc.* **1971**, *93*, 5687. (b) Young, D. A. T.; Willey, G. R.; Hawthorne, M. F.; Churchill, M. R.; Reis, A. H., Jr. *J. Am. Chem. Soc.* **1970**, *92*, 6663. (c) Churchill, M. R.; Reis, A. H., Jr.; Young, D. A. T.; Willey, G. R.; Hawthorne, M. F. *J. Chem. Soc. D* **1971**, 298. (d) Rees, W. S., Jr.; Schubert, D. M.; Knobler, C. B.; Hawthorne, M. F. *J. Am. Chem. Soc.* **1986**, *108*, 5367. (e) Schubert, D. M.; Knobler, C. B.; Rees, W. S., Jr.; Hawthorne, M. F. *Organometallics* **1987**, *6*, 201. (f) Schubert, D. M.; Knobler, C. B.; Rees, W. S., Jr.; Hawthorne, M. F. *Organometallics* **1987**, *6*, 203. (g) Jutzi, P.; Galow, P. *J. Organomet. Chem.* **1987**, *319*, 139. (h) Magee, C. P.; Sneddon, L. G.; Beer, D. C.; Grimes, R. N. *J. Organomet. Chem.* **1975**, *86*, 159. (i) Sneddon, L. G.; Beck, J. S. *J. Am. Chem. Soc.* **1988**, *110*, 3467.
 (2) (a) Schlesinger, H. I.; Sanderson, R. T.; Burg, A. B. *J. Am. Chem. Soc.* **1939**, *61*, 536. (b) Schlesinger, H. I.; Sanderson, R. T.; Burg, A. B. *J. Am. Chem. Soc.* **1940**, *62*, 342. (c) Price, W. C.; Longuet-Higgins, H. C.; Rice, B.; Young, T. F. *J. Chem. Phys.* **1949**, *17*, 217. (d) Smith, S. H.; Miller, R. R. *J. Am. Chem. Soc.* **1950**, *72*, 1452. (e) Bauer, S. H. *J. Am. Chem. Soc.* **1950**, *72*, 622, 1864. (f) Brokaw, R. S.; Pease, R. N. *J. Am. Chem. Soc.* **1952**, *74*, 1590. (g) Schlesinger, H. I.; Brown, H. C.; Hyde, E. K. *J. Am. Chem. Soc.* **1953**, *75*, 209. (h) Maybury, P. C.; Larrabee, J. C. *Inorg. Chem.* **1963**, *2*, 885. (i) Noth, H.; Ehemann, M. *Chem. Commun.* **1967**, 685. (j) Titov, L. V.; Gavrilova, L. A.; Eremin, E. R.; Mishchenchuk, S. S.; Rosolovskii, V. Ya. *Izv. Akad. Nauk SSSR, Ser. Khim.* **1971**, *6*, 1354. (k) Titov, L. V.; Eremin, E. R.; Gavrilova, L. A.; Rosolovskii, V. Ya. *Izv. Akad. Nauk SSSR, Ser. Khim.* **1970**, *1*, 180.
 (3) (a) Greenwood, N. N.; McGinnety, J. A. *Chem. Commun.* **1965**, 331. (b) Greenwood, N. N.; McGinnety, J. A. *J. Chem. Soc. A* **1966**, 1090. (c) Gaines, D. F.; Borlin, J. *J. Am. Chem. Soc.* **1972**, *94*, 1367. (d) Semenko, K. N.; Kravchenko, O. V. *Dokl. Akad. Nauk SSSR* **1976**, *229*, 1131. (e) Bond, A. C.; Himpfl, F. L., Jr. *J. Am. Chem. Soc.* **1981**, *103*, 1098.